Natural Resources Canada / Ressources naturelles Canada

GEOLOGICAL SURVEY OF CANADA
OPEN FILE 8922

Jura Creek field trip: the drowning unconformity and anoxic sediments at the Devonian-Carboniferous boundary, Alberta

P.B. Kabanov

2022

Canada

ISSN 2816-7155
ISBN 978-066-0-45734-5
Catalogue No. M183-2/8922E-PDF

GEOLOGICAL SURVEY OF CANADA
OPEN FILE 8922

Jura Creek field trip: the drowning unconformity and anoxic sediments at the Devonian-Carboniferous boundary, Alberta

P.B. Kabanov

2022

Permanent link: https://doi.org/10.4095/330906

This publication is available for free download through GEOSCAN (https://geoscan.nrcan.gc.ca/).

Recommended citation
Kabanov, P.B., 2022. Jura Creek field trip: the drowning unconformity and anoxic sediments at the Devonian-Carboniferous boundary, Alberta. Geological Survey of Canada, Open File 8922, 21 p. https://doi.org/10.4095/330906

Publications in this series have not been edited; they are released as submitted by the author.

Cover photo: type section of the Exshaw Formation at Jura Creek, July 2019, NRCan image 2022-369

INTRODUCTION

The Upper Devonian – Lower Mississippian strata can be accessed with relative ease in the front ranges of the Alberta Rocky Mountains (Figures 1 and 2). Richards et al. (1994, 2005) and Henderson et al. (2009) provide comprehensive guidebooks for these localities including the Jura Creek canyon outcrops. Representative lists of the Devonian-Carboniferous boundary outcrops in the Canadian Rockies can be found in various publications (*e.g.,* Richards et al., 2002; Johnston et al., 2010; Hedhli et al., 2022a), and the tectono-stratigraphic context of these outcrops is illuminated in the comprehensive guidebook of Pattison et al. (2020). The Famennian-age carbonate strata beneath the Devonian-Carboniferous boundary were also a focus of numerous studies (Meijer Drees et al., 1993; Peterhänsel et al., 2001; Peterhänsel and Pratt, 2008; Hedhli et al., 2022a).

Rather than repeating the descriptions of the Jura Creek exposures from aforementioned publications, this guidebook provides an overview of the tectono-stratigraphic context and the present-day condition of these outcrops. The focal point of this excursion is the abrupt surface in the top of the Famennian-age Palliser limestone and the overlying laminated pyritiferous shale of the Exshaw Formation, one of major hydrocarbon sourcerocks in the subsurface of the Western Canadian Sedimentary Basin (WCSB; MacKay and Pedersen, 2022). This stratigraphic succession is one of worldwide records of the global oceanographic and biotic perturbation at the Devonian-Carboniferous boundary known as the Hangenberg event (Kaiser et al., 2016), with a long track of data obtained from the Jura Creek locality (*e.g.,* Macqueen and Sandberg, 1970; Richard and Higgins, 1988; Johnston et al., 2010; Li et al., 2022).

The abrupt Palliser/Exshaw contact at Jura Creek does not bear a physical signature of hiatus, such as subaerial exposure profile, and it is best described as a *drowning uniformity sensu* Schlager (1981, 1989). This term is not popular enough and therefore requires explanation. Drowning unconformities are “maximum flooding surfaces” specific to carbonate platforms. In the subsurface, drowning unconformities usually make excellent seismic reflectors with basinal strata onlapping carbonate slopes and platform tops. On the outcrop or core face, these contacts are characterized by condensed sections (*e.g.,* shell concentrates) and non-deposition surfaces with hardgrounds sometimes impregnated with phosphate and/or glauconite (*e.g.,* Bosellini and Morsilli, 1997; Godet, 2013). The drowning unconformities are within-trend drowning (“flooding”) surfaces in sequence stratigraphy (Catuneanu, 2006). Fundamental genetic difference from subaerial unconformities renders certain reluctance in accepting them as formal sequence boundaries. Schlager (1999) proposes to accommodate drowning unconformities in sequence stratigraphy as Type 3 sequence boundaries.

Factors commonly called upon to explain the demise and drowning of carbonate platforms are rapid relative sea level rise (it was an original interpretation; Schlager, 1981) and/or carbonate production shutoff by eutrophic turbid waters, either loaded with siliciclastics or upwelled from deep ocean (reviews in Godet, 2013 and Kabanov, 2017). Drowning unconformities are usually produced in settings of tectonic subsidence such as extensional rift basins or foreland basins, and active tectonism leading to the rise of oceanographic barrier is frequently seen as a cause of water column stratification in ancient shelfal basins. Another factor, increasingly recognized in recent years, is the slowdown in ocean circulation under severe global warming, leading to oceanic anoxic events (OAEs), many of which are associated with rapid demise or stepbacks of open-ocean carbonate platforms (*e.g.,* Föllmi and Gainon, 2008; Jenkyns, 2010). Which of these forcings describes the origin of the Palliser/Exshaw contact is still open to a certain degree of conjecture, as briefly reviewed in the last section of this guidebook.

TECTONIC SETTING

The Upper Devonian – Mississippian carbonate succession is part of the overall resistant Late Proterozoic - Paleozoic strata forming the iconic ridges of the Canadian Rockies. These strata are involved in the imbricated system of thin-skinned thrust sheets overthrust upon the Cretaceous foreland siliciclastics during the Laramide Orogeny (Bally et al., 1966; Fermor, 1999; McMechan, 2001; Pattison et al., 2020). Based on $^{40}Ar/^{39}Ar$ dating of thrust gouges, the foreshortening of the western continental margin commenced in the Late Jurassic and proceeded stepwise into Eocene (Pană and van der Pluijm, 2015). The Jura Creek valley is located in the hanging wall of McConnell thrust, one of dominant structures (traced 410 km strike length) separating the front ranges of the Rocky Mountains and the Foothills (Figs. 1 and 2). In the Bow Valley area, including Jura Creek, the displacement relative to the strata in the footwall is estimated at ~40 km (Bally et al., 1966; Fermor, 1999; McMechan, 2001; Pattison et al., 2020). In proximity to Jura Creek, the $^{40}Ar/^{39}Ar$ dating of authigenic illite from the McConnell Thrust gouge provides age ranges of 51.0 ± 3.5 Ma to 57.7 ± 1.2 Ma or late Paleocene to early Eocene (Pană and van der Pluijm, 2015).

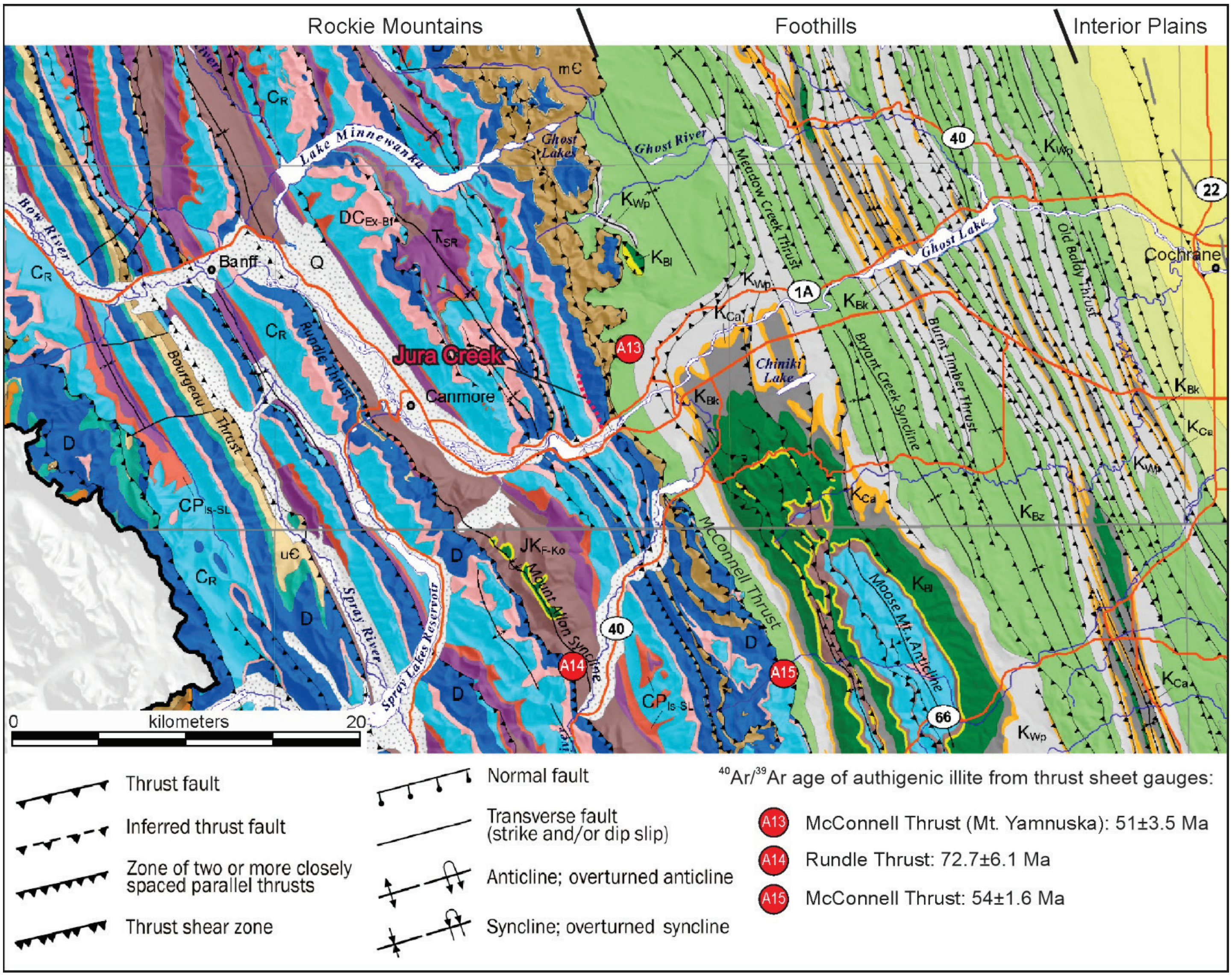

Figure 1. Geological map of the Alberta Rocky Mountains 1:500,000 within NTS map areas 82O-J (Pană and Elgr, 2013); location of Jura Creek outcrops is indicated.

Figure 1 (continued). Bedrock map units (Pană and Elgr, 2013)

Due to heavy overprint of Late Mesozoic - Early Cenozoic tectonism and associated processes, the pre-Laramide geotectonic history of the Canadian Cordillera is generally more open to conjecture (*e.g.,* Johnston, 2008 *vs.*

McMechan et al, 2020). A passive continental margin was established following the late Neoproterozoic – Early Cambrian rifting which broke up Laurentia and a westerly located continental-scale landmass (Colpron et al., 2002; Paradis et al., 2006; Hadlari et al., 2021). Mild synsedimentary deformations affected the western Laurentian margin in southern Canadian Cordillera during the Middle Devonian (Root, 2001). This is interpreted as a response to the early phase of the Antler Orogeny, a time when the shelfal area presently situated in the eastern ranges of the Alberta Rockies was uplifted in the peripheral forebulge (Root, 2001). The Antler Orogeny itself was caused by the docking of Yreka oceanic terrane (in the Roberts Mountains, Nevada). This collision was part of complex Middle Devonian to Mississippian geotectonic processes along the western margin of Laurentia. From present-day Nevada to Yukon and Alaska, the passive-margin regime has apparently changed to a convergent continental margin with an east-verging subduction slab, volcanic arcs, intrusions and effusives. Over the course of Mississippian, rifting in the back-arc seaway has resulted in the opening of Slide Mountain Ocean (Paradis et al., 2006; Colpron and Nelson, 2009; Nelson et al., 2013; Cobbett et al., 2021). In the eastern ranges of the Rocky Mountains, this arc volcanism is manifested in stacked ashbeds found in the Exshaw Formation and younger Early Mississippian strata, including the one confirmed ashbed at Jura Creek (Richards and Higgins, 1988; Richards et al., 1994, 2002; Henderson et al., 2009). Volcanigenic bentonitic seams also occur at the same stratigraphic interval in cores from the Western WCSB (*e.g.,* Smith and Bustin, 2000; Rokosh, 2008; Kabanov et al., 2019).

Detrital zircons from the Devonian-Carboniferous boundary strata, including the Exshaw and Banff formations of Jura Creek and nearby sections, corroborate this big-picture reconstruction by indicating dominance of non-Laurentian age populations derived from terranes of a westerly located oceanic arc (Hedhli et al., 2022b). At the closest reach to the Jura Creek locality, remnants of the Famennian-Tournaisian volcanic arc can be observed in the Kootenay Terrane of SE British Columbia (Richards et al., 2002; Paradis et al., 2006). However, the westerly provenance of clastics in the front ranges of the Alberta Rockies is challenged by very similar detrital zircon age distributions in the Lower Famennian Sassenach Formation of Jasper localities which are likely dominated by the Ellesmerian material from the present-day Canadian Arctics (Hauck et al., 2017).

Figure 2. Views at the front wall of the Rockies from the Willow Rock Campground in Bow Valley. The McConnell Thrust is arrowed. The footwall is the Upper Cretaceous Brazeau Formation; the hanging wall at both cliffs is Middle Cambrian (mainly Eldon Formation). Left: NRCan image 2022-370. Right: NRCan image 2022-371.

LITHOSTRATIGRAPHY

Figure 3 is the cut-out from the Table of Formations representing the Middle Devonian to Mississippian stratigraphy in the central Alberta Rockies and the Foothills (Alberta Geological Survey, 2019 Stratigraphy of two adjacent regions in the subsurface of Western Canada Sedimentary Basin is given for comparison. The grey vertical bar captures stratigraphic succession measured by B.C. Richards at Jura Creek. Descriptions of these sections, in their most recent versions, are available in (Henderson et al., 2009).

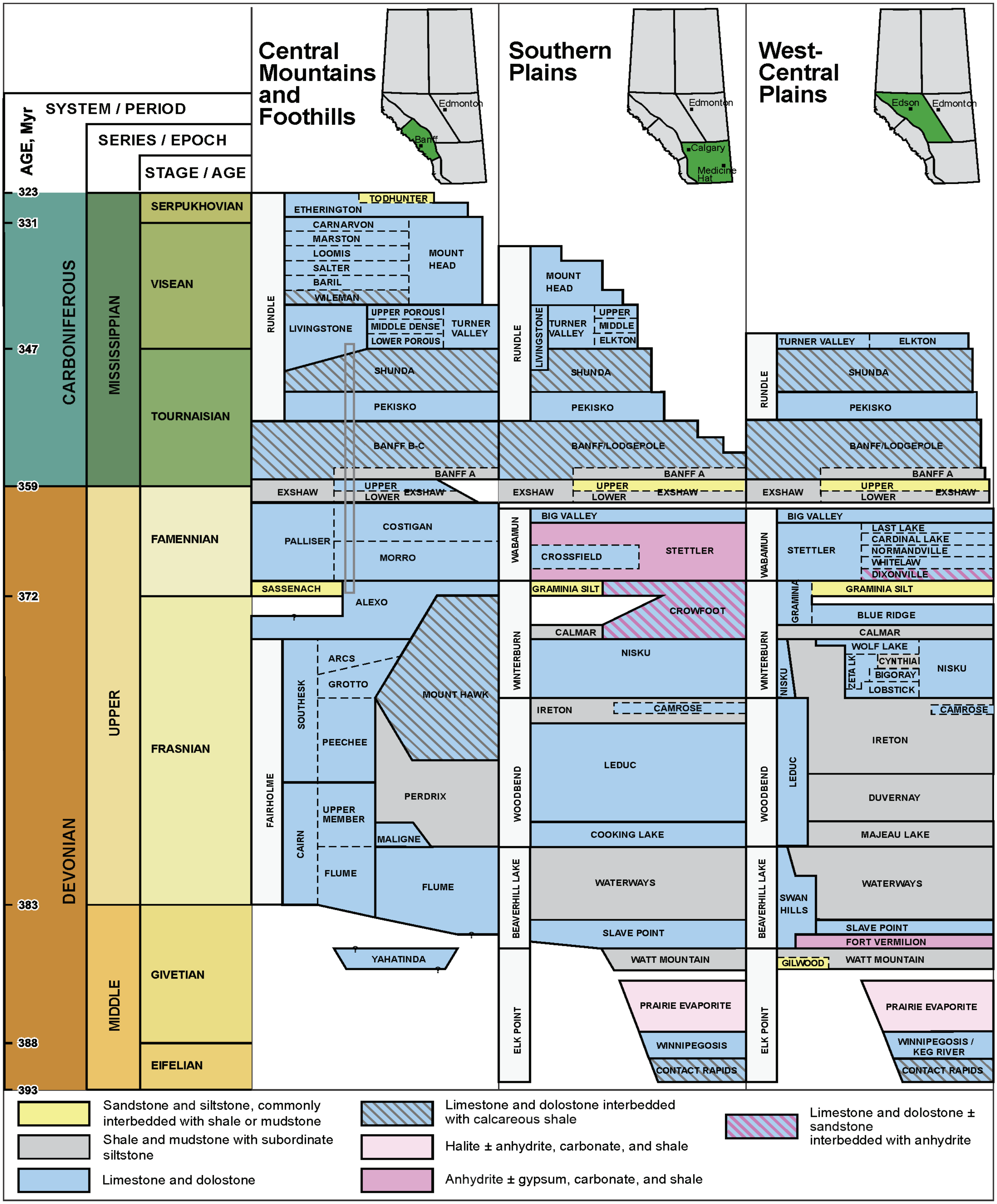

Figure 3. Devonian-Mississippian stratigraphy of the central Alberta Rockies and Foothills region (left column) and adjacent WCSB subsurface (two right columns); Alberta Table of Formations (2019). The grey vertical bar captures stratigraphic succession measured at Jura Creek (Henderson et al., 2009).

JURA CREEK EXPOSURES

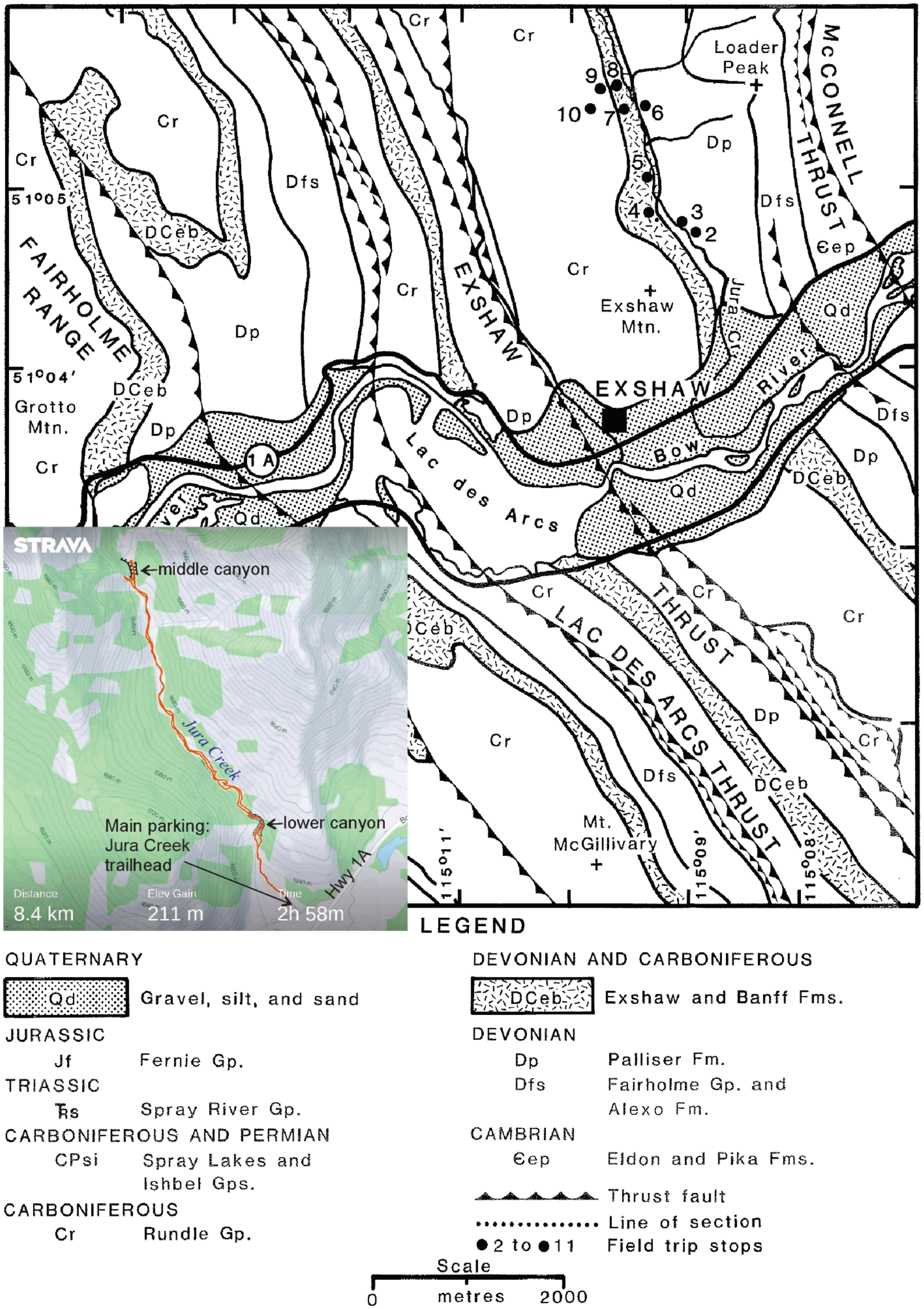

Figure 4. Jura Creek observation stops of B.C. Richards used in a sequence of field trip guidebooks (Richards et al., 1994, 2005; Henderson et al., 2009) on a simplified geologic map; slightly modified from Richards et al. (1994). The inset map is the track to the middle canyon from June 05, 2022.

Out of the published descriptions of geological curiosity hikes along Jura Creek, the one in Henderson et al. (2009) is the most comprehensive and actual to date in its essential details. The trek starts at the recently constructed Jura Creek trailhead parking (Fig. 4). A short walk on a delta fan brings us to the mouth of the lower canyon (Fig. 5A). The middle and lower canyons (inset on Figure 4) are informal appellations for creek bed narrows used in a sequence of published guidebooks (Richards et al., 1994; Henderson et al., 2009). If the creek is dry, it is possible to walk through the canyon to see sedimentary lamination and bioturbation textures on corroded walls of dolomitic limestone of the Morro Member of the Palliser Formation (Fig. 5C,D). If the walk-through is impeded by the stream, it is possible to take the trail that starts on the west bank immediately downstream from the canyon entrance. The trail runs above the western side of the canyon, entering the canyon upstream from the narrows and about 0.5 km downstream from stop 2. A cliff at Stop 2 exposes the upper Morro Member.

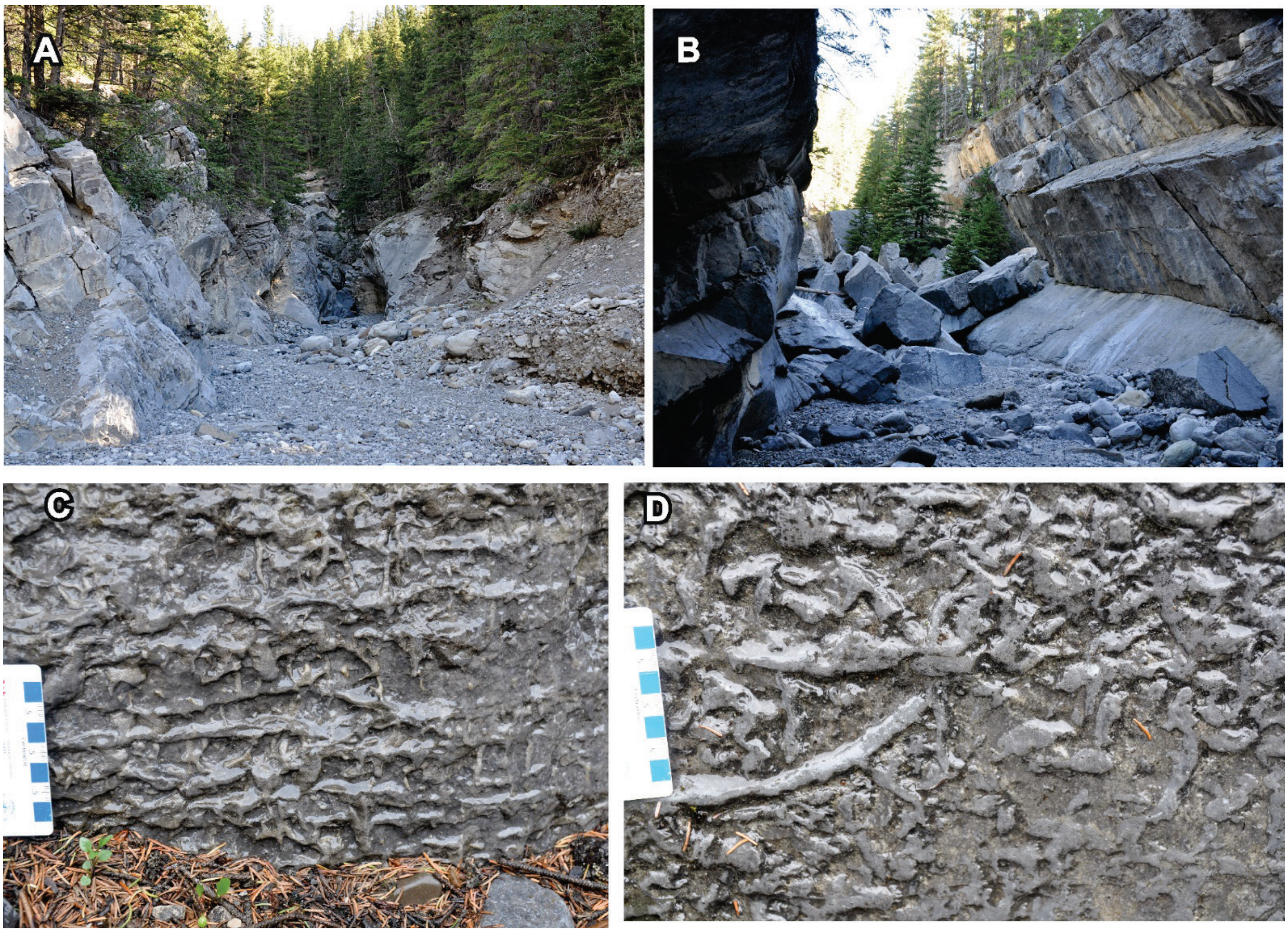

Figure 5. The lower canyon of Jura Creek. **(A)** Mouth of the canyon, NRCan image 2022-372; **(B)** Canyon walls about 100 m upstream of (A) formed by thick-bedded, west-dipping dolomitic limestone of the Morro Member of Palliser Formation, NRCan image 2022-373. **(C, D)** What can be seen on wet walls of the lower canyon: network of burrows and residual sedimentary lamination protruding from corroded limestone walls; (C) NRCan image 2022-374, (D) NRCan image 2022-375.

Upstream from the lower canyon, Jura Creek widens into an easily walkable valley. Creekside outcrops between stops 2 and 4 exhibit many features of the peritidal unit of the Costigan Member (Figs. 6 and 7). Figure 6 is the interpretation of the section compiled by B.C. Richards between his stops 2-4 (Henderson et al., 2009). This section represents about one-half of the Costigan Member; its full thickness is 39.5 m at the stratotype of this unit on Mount Costigan south face located 21.0 km NW of the Jura Creek middle canyon.

Further upstream near stop 5, there are easily accessible outcrops of the dolomitic siltstone (partly silty dolostone) of the lower Banff Formation. This is the turbiditic unit with CDE and DE Bouma sequences. As well as convoluted synsedimentary folding (Fig. 8). The Banff Formation is described in (Henderson et al., 2009). Small isolated exposures of the lithologically similar upper Exshaw and lower Banff formations can be encountered further upstream in the creek bed, including those uncovered during the flood of 2013.

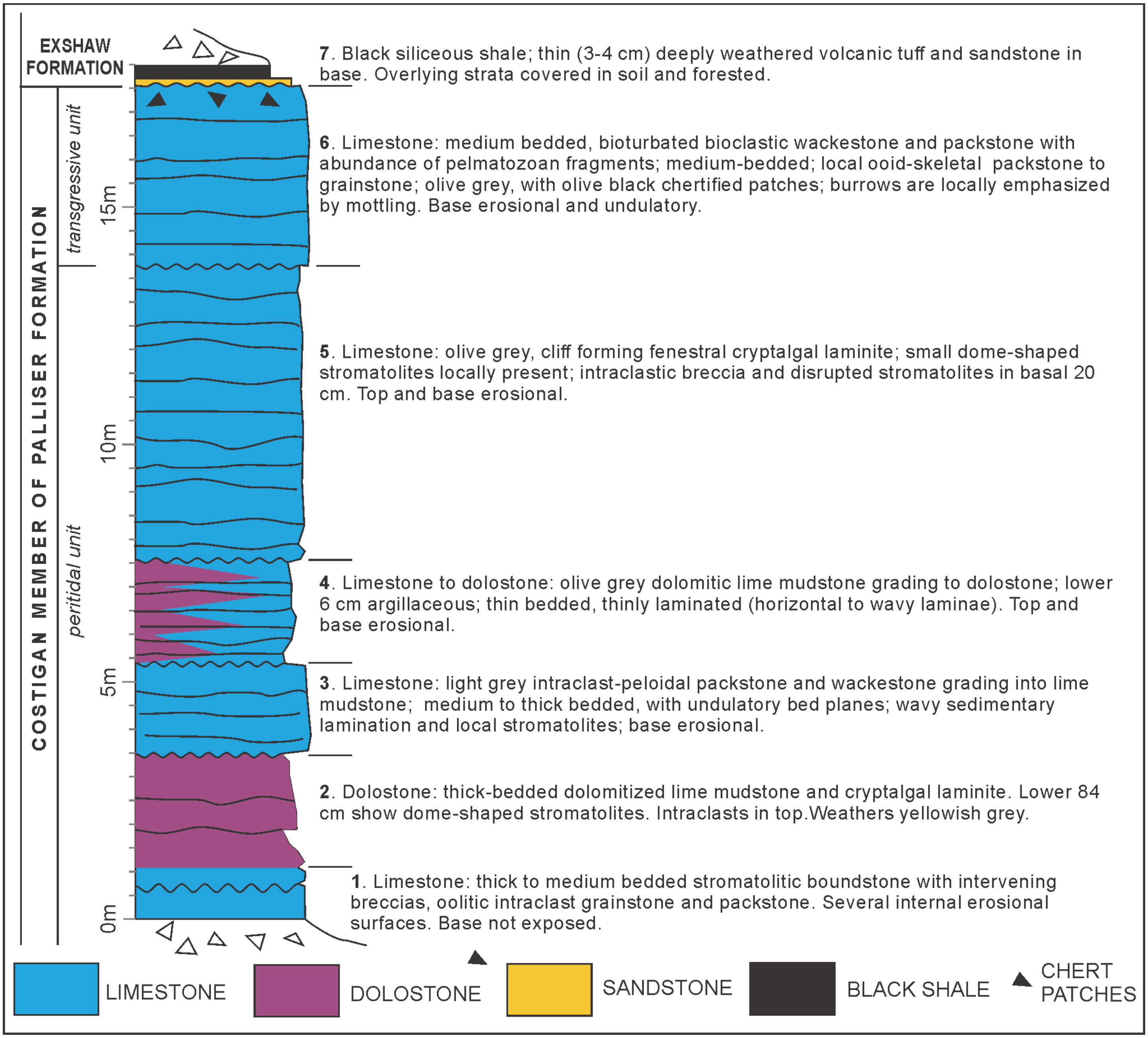

Figure 6. Section of the upper portion of Costigan Member at stops 2-4 (interpreted from figure 27 in Henderson et al., 2009).

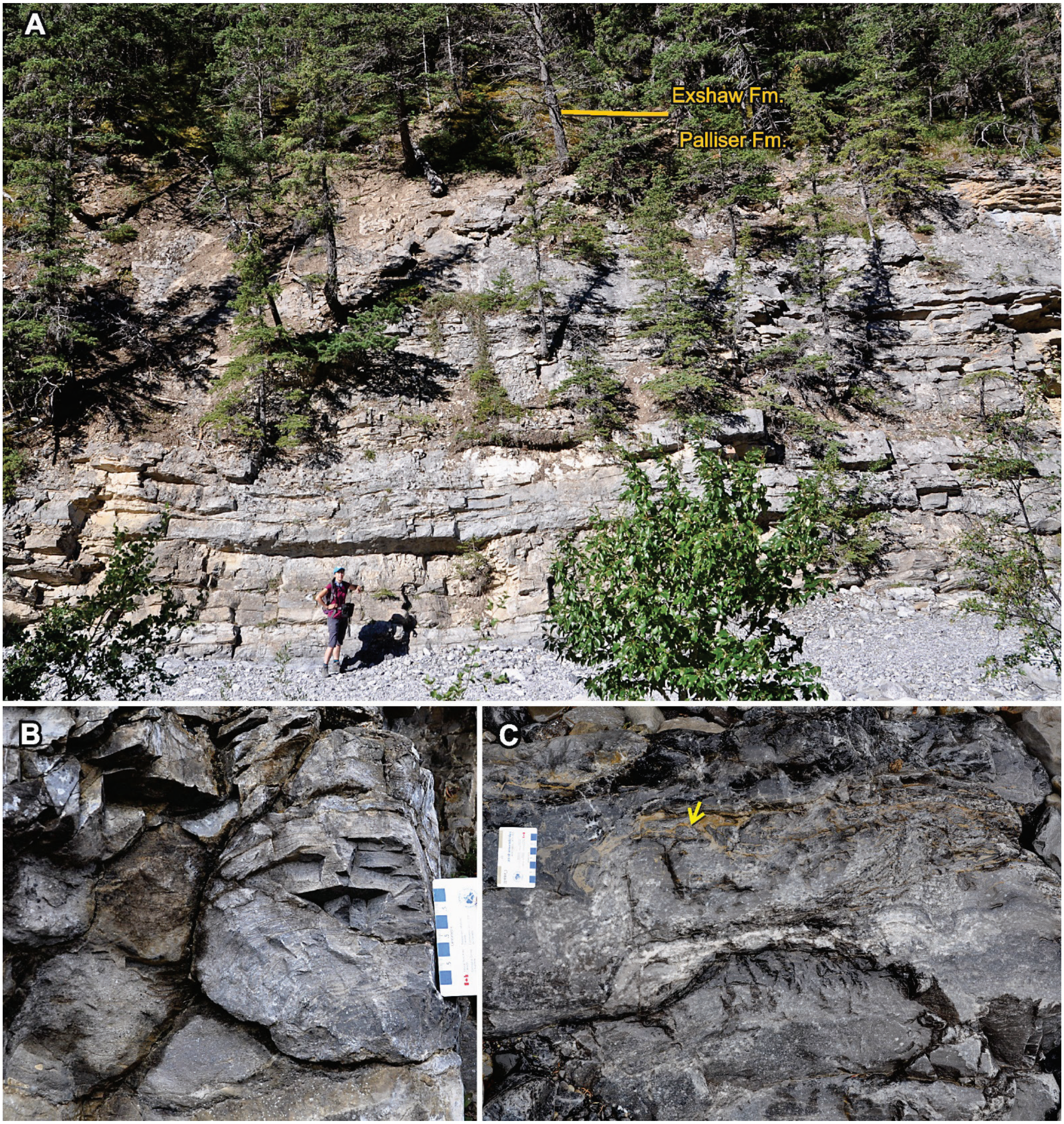

Figure 7. Upstream of the lower canyon, near stop 4 (reference to Figure 4). **(A)** Condition of the Costigan Member outcrop in 2022 (*cf.* figure 26 in Henderson et al., 2009); approximate Palliser/Exshaw contact is indicated; NRCan image 2022-376. **(B)** A stromatolite head in the peritidal unit of the Costigan Member, NRCan image 2022-377; **(C)** wet surface in the same unit allows to see stromatolite which is brecciated from the top (arrow), NRCan image 2022-378.

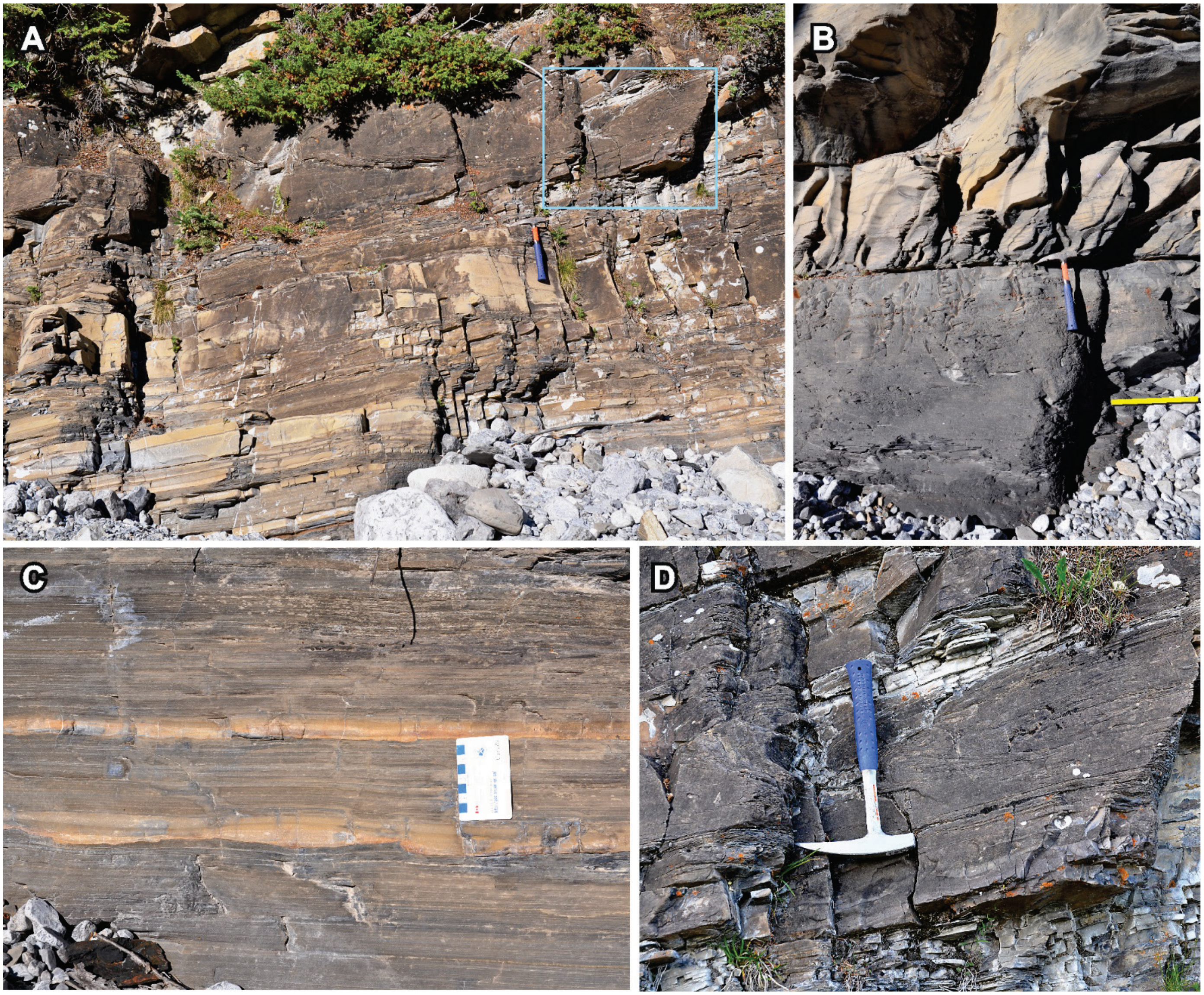

Figure 8. Outcrops at and near stop 5. **(A)** An outcrop of the basal Banff strata at stop 5 showing vivid turbiditic rhythmicity in the basal portion and convoluted lamination in the siltstone above, NRCan image 2022-379; blue box outlines Figure 8D. **(B)** Gradational contact of the lower and upper members of the Exshaw Formation (approximate position traced by yellow line); hammer points at the thin soft shale separating units 6 and 7 in the section description (Figure 9); NRCan image 2022-380. **(C)** Fine-grained graded beds (CDE and DE Bouma sequences) in the basal portion of the Banff Formation interpreted as distal turbidites (Richards et al., 1994; Henderson et al., 2009); NRCan image 2022-381. **(D)** Zoom-in at the blue box on (A) showing convoluted bedding with rolls, an indication of downslope slumping according to B.C. Richards; NRCan image 2022-382.

The type section of the Exshaw Formation is exposed in the so-called middle canyon of Jura Creek (Figs. 9 and 10). This canyon (stops 6-7 of B.C. Richards; Fig. 4) also avails an excellent exposure of the upper portion of Costigan Member and its contact with the Exshaw Formation (Fig. 10). The section description on Figure 9 is based mainly on the comprehensive descriptions of B.C. Richards (Richards et al., 1994, 2002; Henderson et al., 2009), aided by details from the recent microfacies/lithofacies study of M. Hedhli and co-authors (Hedhli, 2019; Hedhli et al., 2022a; Li et al., 2022), as well as author's personal observations. The unit numbering and section meterage is retained from the descriptions of B.C. Richards. The conodont zonation is the interpretation of D.C. Johnston in (Henderson et al., 2009; Johnston et al., 2010). This zonation is interpolated to Jura Creek based on absolute age and biostratigraphic constraints available for the Exshaw Formation in the region. Unfortunately, repeated attempts to extract conodonts from the type Exshaw section have seen only limited success to date.

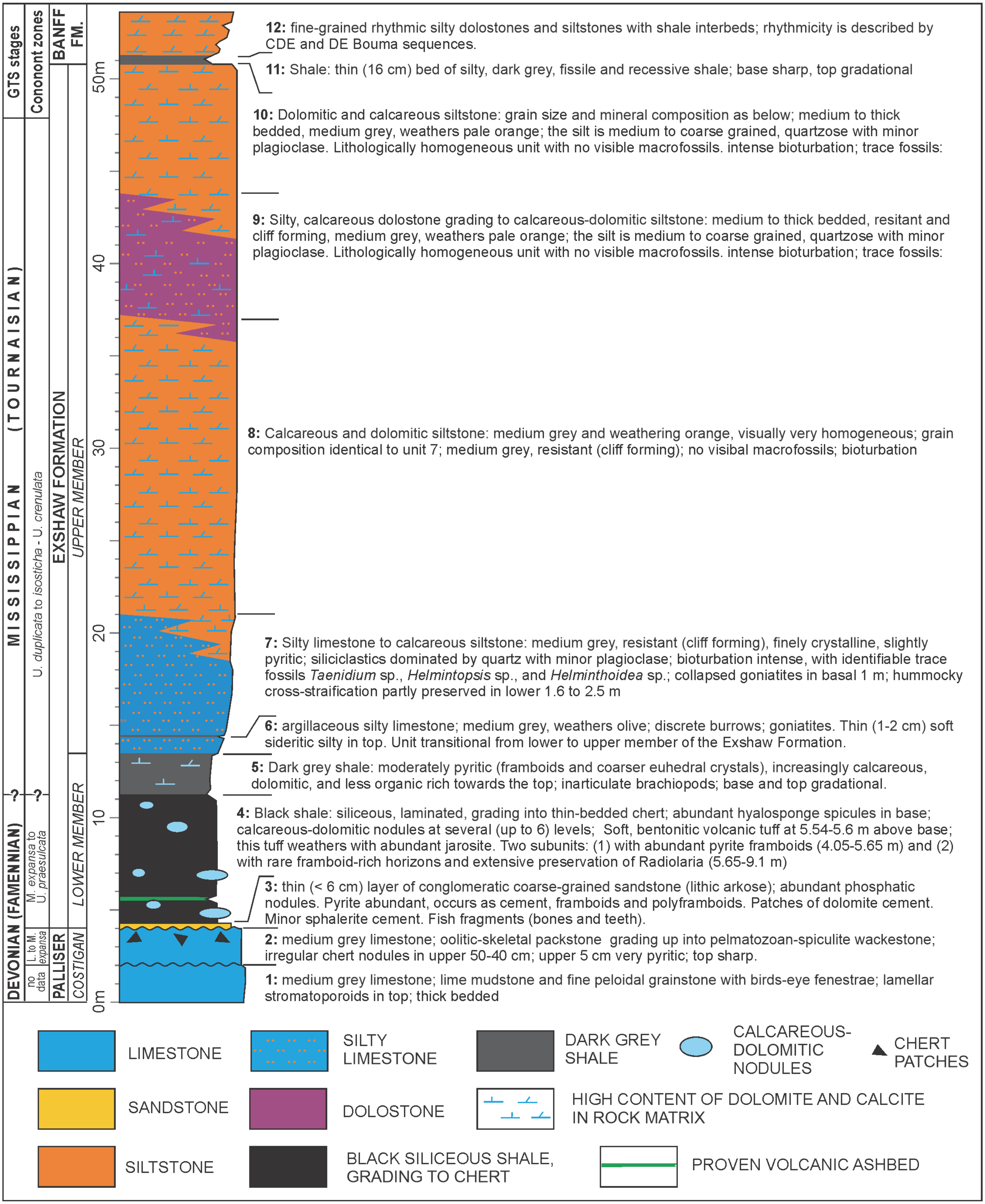

Figure 9. The type section of the Exshaw Formation in the middle canyon of Jura Creek; interpreted from figure 10 in Richards et al. (2002) and figure 32 in Henderson et al. (2009).

Figure 10. The Palliser/Exshaw contact and the lower Exshaw shale in the middle canyon. Units 2,3, and 4 refer to the section on Figure 9. (**A)** Iconic view on the canyon taken in 2019; yellow arrows on forefront point at the gradational contact of the upper and lower members of Exshaw Formation; NRCan image 2022-369. **(B)** Near-planar view at top of the Costigan limestone and the basal Exshaw sandstone; NRCan image 2022-383. **(C)** Bedding-parallel view at the Palliser/Exshaw contact; NRCan image 2022-384. **(D)** Process of acquiring gamma spectrometry data through the lower Exshaw shale; NRCan image 2022-385. Labels: *ch* – chert patches in limestone; *ph* – phosphate nodules; *nod* – authigenic carbonate nodules in the lower Exshaw shale. The ashbed in (A) and (D) is red-arrowed (absolute age data in Richards et al., 2002).

The overlying strata of the upper Exshaw and Banff formations represent the overall shallowing-upward succession (Fig. 11). The content of fine siliciclastics gradually decreases up the section, while the carbonate content increases, including bioclastic material from typical benthic organisms (bryozoans, echinoderms, brachiopods, etc.). Textures indicative of deep-water slope deposition (fine turbiditic rhythmicity, slumping folds) disappear at 113.0 m of the section (lower 62 m of Banff Formation), and the degree of bioturbation increases inversely (Henderson et al., 2009). A detailed section of the Banff Formation and Rundle Group up to the basal portion of the Livingstone Formation was measured by B.C. Richards above the middle canyon (their stops 8 to

10; Henderson et al., 2009). The middle-upper Banff Formation and the fossiliferous limestones of the Rundle Group are interpreted by these authors as the carbonate-ramp to slope deposits (*ibid.*).

Figure 11. The Banff Formation and the overlying limestones of the Rundle Group seen from the mouth of the side canyon of Jura Creek (measured by B.C. Richards at stops 8-10; Fig. 4). Stratigraphy is interpreted on the left (southern) slope of the gully; note the distant traceability of the darker colored Shunda Formation. NRCan image 2022-386.

REDOX CHANGES THROUGH LOWER EXSHAW SHALE

Li et al. (2022) provided the most recent interpretation of the redox changes across the Palliser/Exshaw contact and though the lower Exshaw shale based on their data on pyrite framboid distribution, iron speciation, elemental chemostratigraphy, and microfacies at the Jura Creek location. Author's gamma spectrometry data (Figure 12) are consistent with the redox history presented by Li et al. (2022). These gamma spectrometry readings were acquired with RS-230 BGO scintillometer during two visits in 2019 and 2022 and are presented here for the first time. The signal acquisition time was set to 2 minutes.

Proxies on Figure 12B are calculated as follows:

$$SGR[gAPI] = 8 \times U[ppm] + 4 \times Th[ppm] + 16 \times K[\%] \quad (1)$$

$$KTH[gAPI] = 4 \times Th[ppm] + 16 \times K[\%] \quad (2)$$

$$U_{aut}[ppm] = U[ppm] - Th[ppm] / 3 \quad (3)$$

The SGR (1) is a popular approximation to the total gamma-ray response in API units, and KTH (2) is a uranium-stripped K-Th signal characterizing siliciclastic input (Ellis and Singer, 2008). The KTH is also referred to as CGS (computed or clay gamma-ray) in many works (*ibid.*). Application of these two proxies to the Middle Paleozoic black shales of the northern WCSB was repeatedly discussed (*e.g.,* Kabanov et al., 2019; Kabanov and

Gouwy, 2020). The U_{aut} (3), or authigenic uranium, is a proxy to the excess of uranium (Myers and Wignall, 1987) which in shales with $U_{aut} > 0$ is interpreted as the authigenic enrichment above the U content in detrital minerals (*ibid.*).

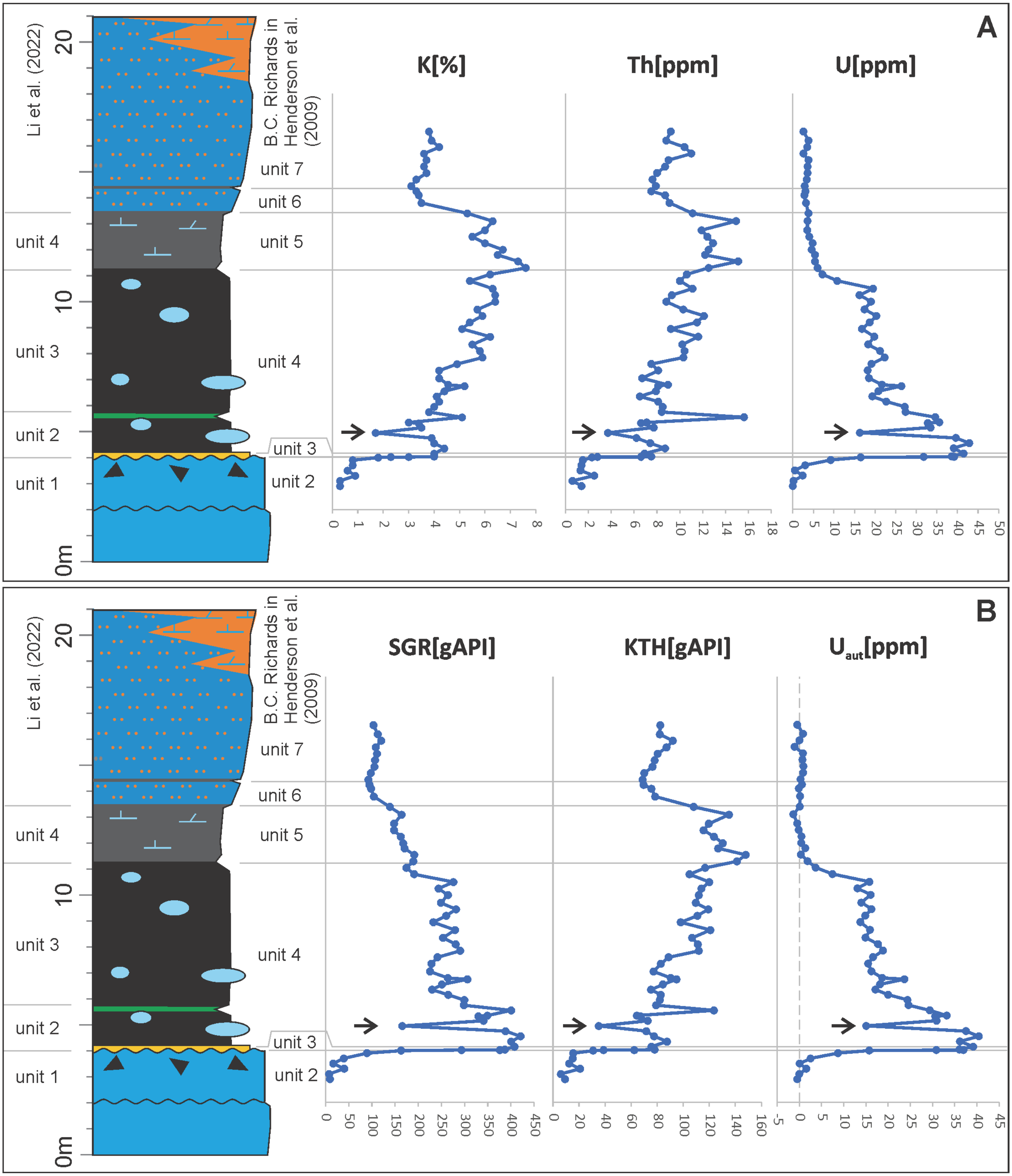

Figure 12. Gamma spectrometry of the type Exshaw section (legend on Figure 9): **(A)** instrumental calculations of elemental concentration; **(B)** redox proxies. Arrows point at the off-trend reading at a large carbonate nodule.

The redox stratigraphy is summarised following meterage and unit numbering of B.C. Richards, in the same way as in the description of this section (Figure 9). Li et al. (2022) devised their own reference units which are also shown on Figure 12.

The uppermost portion of the Palliser Formation (upper unit of Costigan Member) was deposited in a well-oxygenated, relatively oligotrophic setting prerequisite to benthic carbonate production, as indicated by occurrence of crinoidal wackestone and packstone (Peterhansal et al., 2008; Hedhli et al, 2022b) and essential lack of siliciclastics (characterized by low KTH on Figure 12B). The abrupt surface in the Palliser top and incursion of a thin sandstone (unit 3) corresponds to the episode of non-deposition coupled with reworking of lag sediments and extensive phosphogenesis. Severe anoxia with signatures of euxinic condition below the sediment-water interface established following the episode of phosphate growth (Caplan and Bustin 1999; Li et al., 2022), which is consistent with the highest U enrichment in the basal 1.8 m of the lower Exshaw shale. This basal part of the unit 4 of B.C. Richards corresponds to the unit 2 of Li et al. (2022). The overlying portion of the lower Exshaw shale (upper unit 4 of B.C. Richards) records anoxic ferruginous conditions with intermediate concentrations of Mo and U (approximated by U_{aut} on Figure 12). The TOC content in the entire unit 4 varies within the narrow range 3.7-5.0 wt.% and declines to low values of < 2.5 wt.% on transition to unit 5 (Li et al., 2022). The shale of the unit 5 is characterized by the highest concentration of fine siliciclastics (KTH on Figure 12B), correspondingly with its soft, recessive outcrop character indicative of high clay content. Redox-sensitive trace metals (U, Mo, V, Re) decline to sub-oxic levels with practically no authigenic enrichment, and progressive ventilation of the seafloor is also indicated by re-entry of benthic fossils (*e.g.,* inarticulate brachiopods) and bioclasts in thin sections (Richards and Higgins 1988; Li et al., 2022). The existent correlations thus indicate an improved seafloor oxygenation by the time of Hangenberg anoxic event (middle *praesulcata* conodont Zone; (Kaiser et al., 2016), prompting an inquiry into whether the shutdown of benthic carbonate production and the following anoxic pulse of the basal Exshaw, on one hand, and the Hangenberg Shale, on another, record the same oceanographic event (Li et al., 2022).

NATURE OF PALLISER/EXSHAW CONTACT

Table 1 is a brief overview of interpretations of the Palliser/Exshaw contact, which is part of the profound change in depositional environments across the Devonian-Carboniferous boundary traced along the western margin of Laurentia.

Table 1. Interpretations of depositional environments across the Devonian-Carboniferous boundary

Macqueen and Sandberg, 1970	Lagoonal deposition of black shale ("Exshaw lagoons") possibly in shallow depresions produced by gentle tectonic warping of Palliser-Wabamun seafloor. Authors admitted widespread occurrence of similar black shales at the same stratigraphic level across North America.
Richards and Higgins, 1988	The black shale of the lower Exshaw is a deep water sediment. The upper Costigan limestone (transgressive unit) and the basal Exshaw shale are within one transgressive tract; highstand level to be sought within the lower Exshaw. The Costigan/Exshaw contact is a disconformity resulting from minor submarine erosion or nondeposition.
B.C. Richards in Richards et al., 1994, 2005; Henderson et al., 2009	The Costigan/Exshaw contact at Jura Creek is a conformity within the deepening trend of a major Late Famennian eustatic sea level rise. Some erosion is possible at this boundary on regional scale. The Exshaw black shale deposited on a drowned carbonate shelf in deep water (not more than 300 m) anoxic environment. Oceanic upwelling could have controlled high primary production.
Savoy, 1992; Savoy and Mountjoy, 1995; Savoy et al., 2000	Impingement of expanded oxygen minimum zone (OMZ) from the ocean combined with downwarping of Palliser carbonate platform into Antler foreland basin; eustatic transgression seen as a factor of OMZ expansion
Caplan et al, 1996; Caplan and Bustin, 1999	Drowning surface and Exshaw black shale correspond to global spread of anoxic sediments at the Devonian-Carboniferous boundary (DC). Hence ocean-wide overturn must be involved: intersification of primary production driven by accelerated thermohaline circulation and increased nutrient runoff during Late Famennan-Early Tournaisian glaciation. Sea level changes were not the main driving force.
Caplan and Bustin, 2001	Combination of a physiographic barrier (=Anter Orogen) and sea level changes: bottom oceanic waters did not penetrate into back-barrier basin during lower sea level (benthic carbonate deposition of Palliser/Wabamun); during highstands bottom oceanic waters passed through the barrier and upwelled onto carbonate shelf thus switching benthic carbonate production into pelagic sedimentation.
Hedhli et al., 2022a; Li et al., 2022	Antler orogen is seen as an efficient oceanographic barrier, making oceanic upwelling less likely for a carbonate factory shutdown and phosphogenesis at the Palliser/Exshaw contact. Downwarping of carbonate shelf into foreland basin and nutrient runoff from terrigenous sourceland were likely major controlling factors in spread of bottom anoxia. Climatic cooling and intensification of thermohaline circulation could have played a role in demise of Famennian photozoan carbonate factory characterized by abundant lime mud and peloids.

ACKNOWLEDGEMENTS

This is a contribution to GNES (Geoscience for New Energy Supplies) Program of NRCan with management support from Carl Ozyer. First and foremost, Barry Richards (GSC) is thanked cordially for introducing the author to the Jura Creek locality and the geology of the Rockies front ranges in general. The author is indebted to Markam Hedhli (GSC) for generous advice on regional geology, paleogeographic interpretations, and peer-reviewing this manuscript. Those who provided various help with visits to this locality and manuscript preparation are cordially thanked: Vera Baranova, Kira Roberts, and Ekaterina Ostashevskaya (residents of Bow Valley municipalities), Sofie Gouwy (GSC), and Astrid Arts (Cenovus Energy). As this report deals with one of major WCSB sourcerocks, it is a contribution to the WCSB Atlas 2027 initiative; as it describes an internationally important locality of the Devonian/Carboniferous boundary, it is also part of IGCP-652 Project “Reading geologic time in Palaeozoic sedimentary rocks”.

REFERENCES

Bally, A.W., Gordy, P.L. and Stewart, G.A. 1966. Structure, seismic data, and orogenic evolution of the southern Canadian Rocky Mountains. Bulletin of Canadian Petroleum Geology, v. 14, p. 337-381.

Bosellini, A. and Morsilli, M. 1997. A Lower Cretaceous drowning unconformity on the eastern flank of the Apulia Platform (Gargano Promontory, southern Italy). Cretaceous Research, v. 18, p. 51-61. https://doi.org/10.1006/cres.1996.0049

Catuneanu O. 2006. Principles of Sequence Stratigraphy. Amsterdam, Boston, Heidelberg: Elsevier. 375 p.

Caplan, M.L., Bustin, R.M., Grimm, K.A., 1996. Demise of a Devonian-Carboniferous carbonate ramp by eutrophication. Geology 24, 715–718. https://doi.org/10.1130/0091-7613(1996)024<0715:DOADCC>2.3.CO;2.

Caplan, M.L., Bustin, R.M., 1999. Devonian-Carboniferous Hangenberg mass extinction event, widespread organic-rich mudrock and anoxia: causes and consequences. Palaeogeogr. Palaeoclimatol. Palaeoecol. 148, 187–207. https://doi.org/10.1016/S0031-0182(98)00218-1.

Caplan, M.L., Bustin, R.M., 2001. Palaeoenvironmental and palaeoceanographic controls on black, laminated mudrock deposition: example from Devonian-Carboniferous strata, Alberta, Canada. Sediment. Geol. 145, 45–72. https://doi.org/10.1016/S0037-0738(01)00116-6.

Cobbett, R.N., Colpron, M., Crowley, J.L., Cordey, F., Blodgett, R.B., and Orchard, M.J. 2021. Late Devonian magmatism and clastic deposition in the upper Earn Group (central Yukon, Canada) mark the transition from passive to active margin along western Laurentia. Canadian Journal of Earth Sciences, 58: 471–494. DOI:10.1139/cjes-2020-0161

Colpron, M., Logan, J.M., and Mortensen, J.K. U–Pb zircon age constraint for late Neoproterozoic rifting and initiation of the lower Paleozoic passive margin of western Laurentia. Canadian Journal of Earth Sciences, 39: 133–143 (2002) DOI:10.1139/E01-069

Colpron, M. & Nelson, J.L. 2009. A Palaeozoic Northwest Passage: incursion of Caledonian, Baltican and Siberian terranes into eastern Panthalassa, and the early evolution of the North American Cordillera. In: Cawood, P.A. & Kröner, A. (eds) Earth Accretionary Systems in Space and Time. Geological Society, London, Special Publications, 318, 273–307, https://doi.org/10.1144/SP318.10

Ellis, D.V. and Singer, J.M. 2008. Well logging for earth scientists, 2nd ed., Springer Netherlands. ISBN:978-1-4020-4602-5

Fermor, P.R. 1999. Aspects of the three-dimensional structure of the Alberta Foothills and Front Ranges. Geological Society of America Bulletin, v. 111, p. 317-346. DOI:10.1130/0016-7606(1999)111<0317:AOTTDS>2.3.CO;2

Föllmi, K.B., and Gainon F. 2008. Demise of the northern Tethyan Urgonian carbonate platform and subsequent transition towards pelagic conditions: The sedimentary record of the Col de la Plaine Morte area, central Switzerland. Sedimentary Geology, v. 205, p. 142-159. DOI:10.1016/j.sedgeo.2008.02.005

Godet A. 2013. Drowning unconformities: Palaeoenvironmental significance and involvement of global processes. Sedimentary Geology, v. 293, p. 45-66. DOI:10.1016/j.sedgeo.2013.05.002

Hadlari, T., Arnott, R.W.C., Matthews, W.A., Poulton, T.P., Root, K., and Madronich, L.I. 2021. Provenance of the Incipient Passive Margin of NW Laurentia (Neoproterozoic): Detrital Zircon from Continental Slope and Basin Floor Deposits of the Windermere Supergroup, Southern Canadian Cordillera. Lithosphere, v. 2021, 8356327, 10 pages. https://doi.org/10.2113/2021/8356327

Hauck, T.E., Pană, D., and DuFrane, S.A. 2017. Northern Laurentian provenance for Famennian clastics of the Jasper Basin (Alberta, Canada): A Sm-Nd and U-Pb detrital zircon study. Geosphere, v. 13, no. 4, p. 1149–1172. doi:10.1130/GES01453.1.

Hedhli, M. 2019. Devonian to Carboniferous Earth Systems Change in Western Laurentia (Unpublished doctoral thesis). University of Calgary, Calgary, AB. http://hdl.handle.net/1880/110375

Hedhli, M., Dewing, K., Beauchamp, B., Grasby, S.E., and Meyer, R. 2022a. Devonian to Carboniferous continental-scale carbonate turnover in Western Laurentia (North America): upwelling or climate cooling? Facies, v. 68. https://doi.org/10.1007/s10347-022-00653-4

Hedhli, M., Matthews, W.A., Hadlari, T., Alonso-Torres, D., Grasby, S.E., and Beauchamp, B. 2022b. Detrital Zircon U-Pb Geochronology of Upper Devonian and Lower Carboniferous Strata of Western Laurentia (North America): A Record of Transition from Passive to Convergent Margin. Lithosphere, v. 2022, 9585729, 18 pages. https://doi.org/10.2113/2022/9585729

Henderson, C.M., Richards, B.C., and Johnston, D. 2009. ICOS 2009 Rocky Mountain Fieldtrip. Permophiles (Newsletter of the Subcommission on Permian Stratigraphy) no. 53, Suppl. 2.

Jenkyns, H.C. 2010. Geochemistry of oceanic anoxic events. Geochemistry, Geophysics, Geosystems, v. 11. Q03004. DOI:10.1029/2009GC002788.

Johnston, D. I., Henderson, C. M., and Schmidt, M. J., 2010. Upper Devonian to Lower Mississippian conodont biostratigraphy of uppermost Wabamun Group and Palliser Formation to lowermost Banff and Lodgepole formations, southern Alberta and southeastern British Columbia, Canada: Implications for correlations and sequence stratigraphy. Bulletin of Canadian Petroleum Geology 58: 295-341. DOI:10.2113/gscpgbull.58.4.295

Johnston, S.T. 2008. The Cordilleran ribbon continent of North America. Annual Review of Earth and Planetary Sciences, 36, 495–530. DOI:10.1146/annurev.earth.36.031207.124331

Kabanov, P. 2017. Chapter 6. Stratigraphic unconformities: Review of the concept and examples from the Middle-Upper Paleozoic; In: Aiello, G. (ed.): Seismic and sequence stratigraphy and integrated stratigraphy - New insights and contributions. InTechOpen, p. 101-127. DOI:10.5772/intechopen.70373

Kabanov, P.B. and Gouwy, S.A., 2020. The type section of the Canol Formation (Devonian black shale) at Powell Creek: Critical assessment and correlation in the northern Cordillera, NWT, Canada; Bulletin of Canadian Petroleum Geology, v. 68, p. 123–140 p. DOI:10.35767/gscpgbull.68.4.123

Kabanov, P., Richards, B.C., Hyun Suk Lee, Thapa, P., King, H.M., and Mort, A., 2019. Reference surface and subsurface sections of the Besa River Formation, Liard Basin, British Columbia; Geological Survey of Canada, Open File 8468, 1 .zip file. DOI:10.4095/314567

Kaiser, S.I., Aretz, M., and Becker, R.T., 2016. The global Hangenberg Crisis (Devonian–Carboniferous transition): review of a first-order mass extinction. In: Becker, R. T., Königshof, P. & Brett, C. E. (eds)

Devonian Climate, Sea Level and Evolutionary Events. Geological Society, London, Special Publications, 423, p. 387-437. DOI:10.1144/SP423.9

Li, S., Wignall, P.B., Poulton, S.W., Hedhli, M., and Grasby, S.E. 2022. Carbonate shutdown, phosphogenesis and the variable style of marine anoxia in the late Famennian (Late Devonian) in western Laurentia. Palaeogeography, Palaeoclimatology, Palaeoecology, v. 589, 110835. DOI:10.1016/j.palaeo.2022.110835

MacKay, P. and Pedensen, P. 2022. The Western Canada Sedimentary Basin: A confluence of science, technology, and ideas. AAPG Bulletin, v. 106, p. 655–676. DOI:10.1306/12032121141

Macqueen, R.W. and Sandberg, C.A. 1970. Stratigraphy, age, and interregional correlation of the Exshaw Formation, Alberta Rocky Mountains. Bulletin of Canadian Petroleum Geology, v. 18, p. 32-66.

McMechan, M.E. 2001. Large-scale duplex structures in the McConnell thrust sheet, Rocky Mountains, Southwest Alberta. Bulletin of Canadian Petroleum Geology, v. 49. 408-425.

McMechan, M.E.. Root, K.G., Simony, P.S., and Pattison, D.R.M. 2020. Nailed to the craton: Stratigraphic continuity across the southeastern Canadian Cordillera with tectonic implications for ribbon continent models. Geology, v. 49, p. 101-105. DOI:10.1130/G48060.1

Meijer Drees, N.C., Johnston, D.I., and Richards, B.C. The Devonian Palliser Formation and its equivalents, Southern Alberta, Canada. GSC Open File 2698. DOI:10.4095/193347

Myers, K.J., and Wignall, P.B. 1987. Understanding Jurassic organic-rich mudrocks – New concepts using gamma-ray spectrometry and paleoecology: Examples from the Kimmeridge Clay of Dorset and the Jet Rock of Dorshire. In: Marine Clastic Sedimentology. J.K. Legget and G.G. Zuffa (eds). Graham and Trotman, p. 172–189.

Nelson, J.L., Colpron M., and Israel S., 2013. Chapter 3. The Cordillera of British Columbia, Yukon, and Alaska: Tectonics and Metallogeny. In: M. Colpron, T. Bissig, B.G. Rusk, and J.F.H. Thompson (Eds.), Tectonics, Metallogeny, and Discovery: The North American Cordillera and Similar Accretionary Settings. Society of Economic Geologists, Special Publication. 17, 53–109.

Pană, D.I., and Elgr, R., compilers, 2013, Geology of the Alberta Rocky Mountains and Foothills: Alberta Energy Regulator–Alberta Geological Survey Map 560, scale 1:500,000.

Pană, D.I. and van der Pluijm, B.A. 2015. Orogenic pulses in the Alberta Rocky Mountains: Radiometric dating of major faults and comparison with the regional tectono-stratigraphic record. GSA Bulletin, v. 127, p. 480–502. DOI:10.1130/B31069.1

Paradis, S., Bailey, S.L., Creaser, R.A., Piercey, S.J., and Schiarizza, P., 2006, Paleozoic magmatism and syngenetic massive sulphide deposits of the Eagle Bay assemblage, Kootenay terrane, southern British Columbia, in Colpron, M., and Nelson, J.L., eds., Paleozoic Evolution and Metallogeny of Pericratonic Terranes at the Ancient Pacific Margin of North America, Canadian and Alaskan Cordillera: Geological Association of Canada Special Paper 45, p. 383–414.

Pattison, D.R.M., Moynihan, D.P., McFarlane, C.R.M., Simony, P.S., and Cubley, J.F. 2020. Field guide to the geology, metamorphism and tectonics of the Foreland and Omineca belts of SW Alberta and SE British Columbia. Geological Association of Canada Field Guide Series 2020-A, 257 pp. doi:10.11575/PRISM/38351

Peterhänsel A., Pratt B.R. 2001. Nutrient-triggered bioerosion on a giant carbonate platform masking the post-extinction Famennian benthic community. Geology. v. 29, p. 1079–1082. DOI:10.1130/0091-7613(2001)029<1079:NTBOAG>2.0.CO;2

Peterhänsel, A., Pratt, B.R., and Holmden, C. 2008. The Famennian (Upper Devonian) Palliser Platform of western Canada—architecture and depositional dynamics of a post-extinction epeiric giant. In: Pratt, B.P. and Holmden, C. (eds.), Dynamics of Epeiric Seas, Geol. Assoc. Canada Special Paper 48, p. 247–281.

Richards, B.C. and Higgins, A.C. 1988. Devonian-Carboniferous boundary beds of the Palliser and Exshaw formations at Jura Creek, Rocky Mountains, southwestern Alberta. In: Devonian of the World. N.J. McMillan, A.F. Embry and D.J. Glass (eds.). Canadian Society of Petroleum Geologists, Memoir 14, v. II, p. 399-412.

Richards, B.C., Bamber, E.W., Henderson, C.M., Higgins, A.C., Johnston, D.I., Mamet, B. and Meijer Drees, N.C., 1994. Uppermost Devonian (Famennian) and Lower Carboniferous (Tournaisian) at Jura Creek, and Mount Rundle, Field Trip Guidebook. GSC Open File 2866, 79 p. DOI:10.4095/194058

Richards, B.C., Mamet, B.L. and Bamber. E.W. 2005 Carboniferous sequence stratigraphy, biostratigraphy, and basin development in the vicinity of the Bow Corridor, southwestern Alberta. American Association of Petroleum Geologists Annual Convention, June 19–22 2005 Calgary, Field Trip no. 2 Guidebook, 190 p.

Richards, B.C., Ross, G.M. and Utting, J., 2002. U-Pb geochronology, lithostratigraphy and biostratigraphy of tuff in the upper Famennian to Tournaisian Exshaw Formation: Evidence for a mid-Paleozoic magmatic arc on the northwestern margin of North America. In: L.V. Hills, C.M. Henderson and E.W. Bamber (eds.). Carboniferous and Permian of the World. Canadian Society of Petroleum Geologists Memoir19:158-207.

Rokosh, C.D., Pawlowicz, J.G., Berhane, H., Anderson, S.D.A., and Beaton, A.P. 2008. Geochemical and sedimentological investigation of the Banff and Exshaw Formations for shale gas potential: Initial results. ERCB/AGS Open File Report 2008-10

Root, K.G. 2001. Devonian Antler fold and thrust belt and forelandbasin development in the southern Canadian Cordillera: implications of the Western Canada Sedimentary Basin. Bull. Can. Petrol. Geol. 49: 7–36. DOI:10.2113/49.1.7

Savoy, L.E., 1992, Environmental record of Devonian–Mississippian carbonate and low-oxygen facies transitions, southernmost Canadian Rocky Mountains and northwesternmost Montana. Geological Society of America Bulletin, v. 104, p. 1412–1432. DOI:10.1130/0016-7606(1992)104<1412:ERODMC>2.3.CO;2

Savoy, L.E. and Mountjoy, E.W. 1995. Cratonic-margin and Antler-age foreland basin strata (Middle Devonian to Lower Carboniferous) of the southern Canadian Rocky Mountains and adjacent Plains morphology. In: Stratigraphic Evolution of Foreland Basins. S.L. Dorobek, and G.M. Ross (eds.). Society for Sedimentary Geology, Special Publication No. 52, p. 213-231.

Savoy, L.E., Stevenson, R.K. and Mountjoy, E.W., 2000, Provenance of Upper Devonian–Lower Carboniferous miogeoclinal strata, southeastern Canadian Cordillera: Link between tectonics and sedimentation. Journal of Sedimentary Research, v. 70, p. 181–193. https://doi.org/10.1306/2DC40909-0E47-11D7-8643000102C1865D

Schlager, W., 1981. The paradox of drowned reefs and carbonate platforms. Geological Society of America Bulletin 92, 197–211. DOI:10.1130/0016-7606(1981)92<197:TPODRA>2.0.CO;2

Schlager, W. 1989. Drowning unconformities on carbonate platforms. In: Crevello, P.D., Wilson, J.L.,.Sarg, J.F., Read, J.F. (editors). Controls on Carbonate Platform and Basin Development.Society of Economic Paleontologists and Mineralogists Special Publication 41. pp. 15-25.

Schlager, W. 1999. Type 3 sequence boundaries. In: Harris PM, Saller AH, Simo JA, editors. Advances in Carbonate Sequence Stratigraphy: Application to Reservoirs, Outcrops, and Models. Vol. 63. Society of Economic Paleontologists and Mineralogists, Special Publication. Tulsa, OK: SEPM, 1999. pp. 35-46.

Smith, M.G. and Bustin, R.M. 2000. Late Devonian and Early Mississippian Bakken and Exshaw Black Shale Source Rocks, Western Canada Sedimentary Basin: A Sequence Stratigraphic Interpretation. AAPG Bulletin, 84: 940–960. DOI:10.1306/A9673B76-1738-11D7-8645000102C1865D